

Spatio-Temporal Analysis of Shoreline Changes and Wave Modeling: Case of Mostaganem Bay, Algeria

Prostorno-vremenska analiza promjena obalne linije i modeliranje valova: slučaj zaljeva Mostaganem, Alžir

Miloud Sallaye*

Institute of Architecture and Earth Sciences
University of Ferhat Abbas Setif 1
Setif, Algeria
E-mail: sallaye.miloud@univ-setif.dz

Abd El Alim Dahmani

National School of Marine Science and
Coastal Planning (ENSSMAL) Algiers,
Algeria
E-mail: dahmani.abdelalim@gmail.com

Yousra Salem Cherif

National School of Marine Science
and Coastal Planning (ENSSMAL)
Algiers, Algeria
E-mail: yousra.sc@gmail.com

Khoudir Mezouar

National School of Marine Science
and Coastal Planning (ENSSMAL)
Algiers, Algeria
E-mail: mezouarkhoudir@yahoo.fr

DOI 10.17818/NM/2025/1.1

UDK 551.35.054:551.468.2(65)

Original scientific paper / Izvorni znanstveni rad

Paper received / Rukopis primljen: 26. 3. 2024.

Paper accepted / Rukopis prihvaćen: 21. 11. 2024.



This work is licensed under a
Creative Commons Attribution
4.0 International License.

Abstract

The coastal area of Mostaganem, from Sidi Madjedoub in the east to Oureah in the west, is a very interesting and remarkable place. Over the last 20 years, it has been exposed to a series of natural and anthropogenic processes that generate both short- and long-term variations of the shoreline position. This research is based on a spatial-temporal analysis of shoreline change along the coast between Sidi Madjedoub and Oureah, using aerial photographs from 2003 and QuickBird satellite images from 2014 and 2023. The use of Geographic Information Systems (GIS) and the Digital Shoreline Analysis System (DSAS) geostatistical tool enabled the identification of erosion and accretion rates, as well as the description of evolutionary trends over a 20-year, covering three periods (2003–2014, 2014–2023, and 2003–2023). The shoreline changes were calculated using 720 transects generated at 20-meter intervals. In addition, numerical modeling of wave propagation was carried out using the Mike 21 model to gain a better understanding of the influence of coastal hydrodynamics on shoreline change. The results reveal that most of the studied area is experiencing erosion, with an average rate of -0.28 meters per year along the entire coast. These changes result basically from sea-level rise and longshore sediment transport generated by the waves and currents approaching mostly from NNE quadrant, and human activities (sand mining, urbanization, touristic activities). This study demonstrates that combined use of satellite imagery and statistical method such as linear regression for shoreline change analysis are helpful for erosion monitoring and preventive measure.

Sažetak

Obalno područje Mostaganema, od Sidi Madjedouba na istoku do Oureaha na zapadu, vrlo je zanimljivo i značajno područje. Tijekom posljednjih 20 godina bilo je izloženo brojnim prirodnim i antropogenim procesima koji su uzrokovali kratkoročne i dugoročne promjene položaja obalne linije. Istraživanje se temelji na prostorno-vremenskoj analizi promjene obalne linije duž obale između Sidi Madjedouba i Oureaha, korištenjem fotografijama iz zraka 2003. godine te QuickBird satelitskih snimki iz 2014. i 2023. godine. Korištenjem geografskim informacijskim sustavom (GIS) i geostatičkim alatima – digitalnim sustavima za analizu obale (DSAS) identificirane su stope erozije i akumulacije te opisani evolucijski trendovi tijekom 20 godina, što obuhvaća tri razdoblja (2003. – 2014., 2014. – 2023. i 2003. – 2023.). Promjene obalne linije izračunate su na temelju 720 transekata generiranih u razmacima od 20 metara. Osim toga, provedeno je numeričko modeliranje širenja valova s pomoću modela Mike 21 kako bi se bolje razumio utjecaj obalne hidrodinamike na promjenu obalne linije. Rezultati pokazuju da je veći dio istraživanih područja podložan eroziji, s prosječnom stopom od -0,28 metara godišnje duž cijele obale. Te su promjene prvenstveno rezultat porasta razine mora i obalnog transporta sedimenta uzrokovanog valovima i strujama koji se uglavnom približavaju iz NNE kvadranta, kao i ljudskih aktivnosti (iskopavanje pijeska, urbanizacija, turističke aktivnosti). Ovaj rad pokazuje kako je kombinirana upotreba satelitskih snimaka i statističkih metoda, poput linearne regresije za analizu promjena obalne linije, korisna za praćenje erozije i provedbu preventivnih mjera.

KEY WORDS

Erosion
GIS
DSAS
Mike 21
Coastal hydrodynamic

KLJUČNE RIJEČI

erozija
GIS
DSAS
Mike 21
obalna hidrodinamika

* Corresponding author

1. INTRODUCTION / Uvod

The vulnerability of Mediterranean coastlines is increasing due to the growing combined pressures of human activities and environmental hazards [1-3]. The northern Algerian coast, like other coastal areas around the world, is susceptible to rapid economic activities associated with a significant increase in demographic pressure and unregulated use of resources [4-5].

Coastal degradation is one of the main challenges facing coastal systems. Coastal erosion degrades the quality of ecosystems formed by ecotones that separate land from sea [6].

The shoreline, marking the boundary between land and sea, is considered one of the most intricate, dynamic, and unstable geomorphological elements of the coastal system [7], influenced by both terrestrial and marine forces [8-11]. Changes in the shoreline are regarded as essential indicators of coastal erosion risk [12]. Numerous studies highlight that shoreline alterations can be attributed to two primary factors: anthropogenic activities along the coast and natural phenomena such as littoral transport, tidal surges, waves, and storms [13-16]. The technique of shoreline evolution assessment has become an effective means of evaluating spatial and temporal variations in beach accretion and erosion [17-19]. Therefore, coastal resource management, sustainable coastal development, and coastal conservation rely heavily on accurate, up-to-date shoreline maps and continuous monitoring [20].

Many scientists have utilized the Digital Shoreline Analysis System (DSAS) to assess shoreline variations along the Algerian coast [21-24]. During the last decade, the western region of Algeria, particularly the Mostaganem coast, has experienced rapid development due to tourism, economic expansion, and coastal development projects such as coastal protection

structures, major ports, and minor ports [25]. On a smaller scale, the coastal area from Sidi Madjedoub to Oureah Beach is a favorite among tourists and serves as a source of funding for the local community. However, this coastal zone has been affected by soil degradation, erosion, water pollution, and flooding [26]. These significant fluctuations are particularly evident along the sandy coasts, such as Metarba Beach and Salamander Beach.

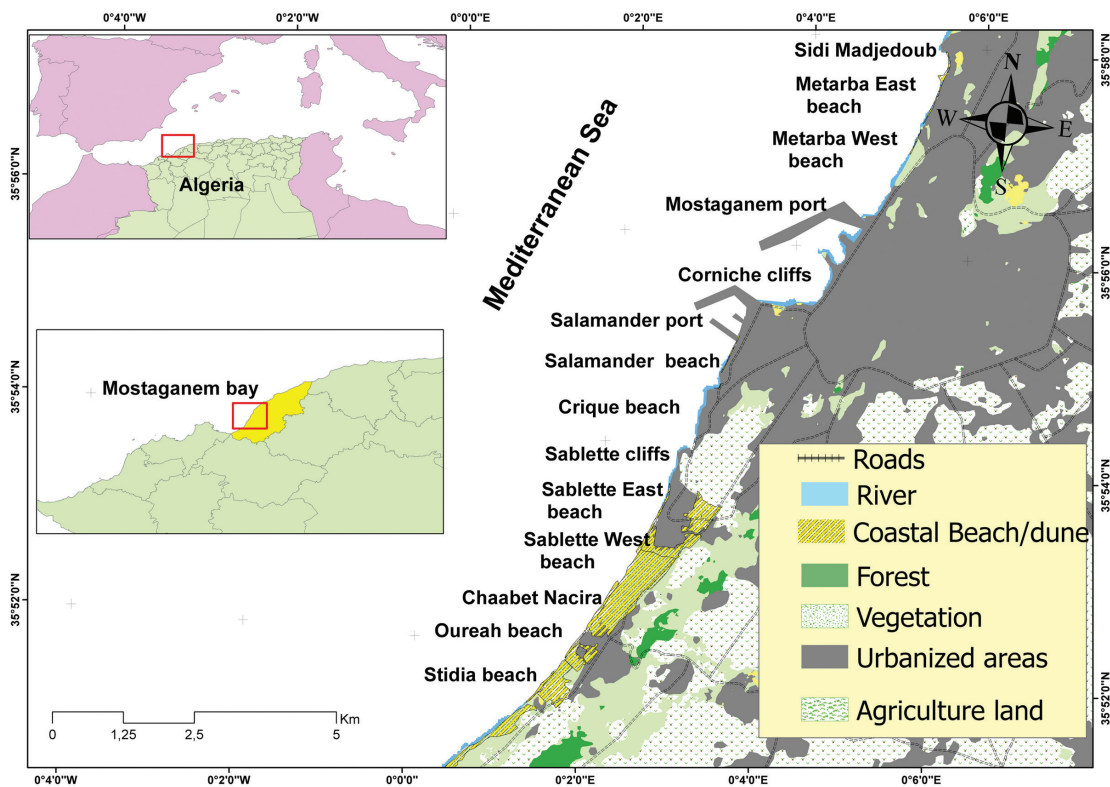
This study has shown the trends in shoreline evolution and the factors influencing these variations. Aerial photographs taken in 2003 and satellite images from 2014 and 2023 were used to digitize the shoreline. The use of GIS can provide valuable information's on changes to the shoreline and coastal degradation. The Digital Shoreline Analysis System (DSAS) on the ArcGIS platform was applied to generate statistical analyses of the shoreline and transects.

To better understand the longshore dynamics in the study area, the MIKE 21 model was applied to simulate the hydrodynamic conditions.

For this purpose, the objectives of our study are to understand the historical shoreline changes along the Mostaganem coastline from 2003 to 2023, assess the negative impacts of new constructions in the area, and analyze the main factors influencing shoreline evolution.

2. STUDY AREA / Područje istraživanja

The study area extends approximately 15 km along the western littoral of Algeria, situated between Sidi Madjedoub in the east and Oureah in the west. The geographical coordinates of the study area range between latitudes 35°52'00"N to 35°58'45"N and longitudes 0°2'0"W to 0°6'0"E (Figure 1).



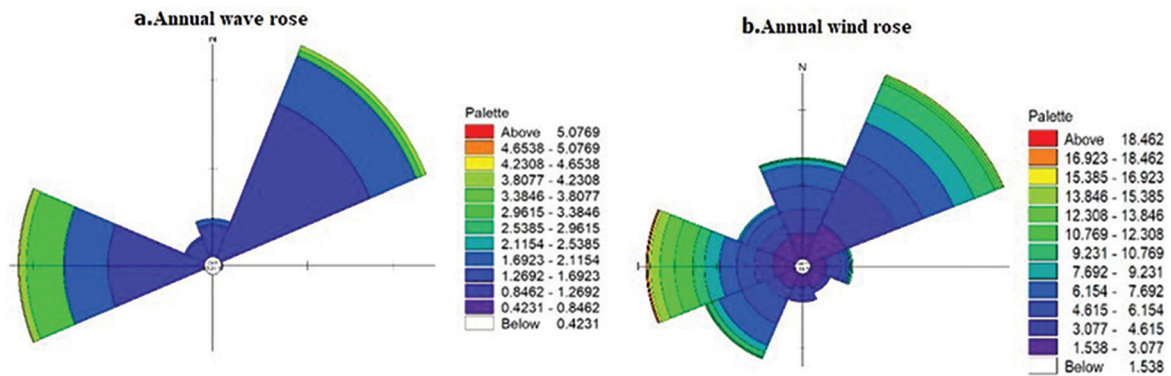


Figure 2 Annual wave rose and annual wind rose 2020 [27].
Slika 2. Godišnja ruža valova i godišnja ruža vjetrova 2020.

The study area is situated within a semi-arid Mediterranean climate, which is defined by distinct seasonal variations. It is characterized by a short, mild, rainy winter and a long, hot, dry summer. Wind and wave data were collected from the Infoplaza Marin database [27]. The most frequent winds are from the west and south-west in winter and from the north and northeast in summer.

Statistical data reveal that wave conditions in the study area fluctuate with the seasons; the predominant waves originate from the north-northeast direction, with periods ranging from 8 to 10 seconds, while those from the west have periods between 7 and 8 seconds. These directions inducing prominent morphological changes because they also coincide with the highest and most energetic waves occurring in winter (Figure 2). The tidal pattern along the Mediterranean coast of Algeria is predominantly semidiurnal and characterised by a relatively minor impact, with a mean tidal range between 25 to 70 cm. Additionally, two major coastal structures have been constructed along the coastal in the study area: Mostaganem port in 1905 and Salamander port in 2003 [28].

3. MATERIALS AND METHODS / Materijali i metode

3.1. Data Sources / Izvori podataka

Shoreline changes were analyzed using aerial imagery acquired in 2003 and QuickBird satellites imagery from 2014 and 2023, with a spatial resolution of 0.5 m (Table 1). Mosaic processing, geodatabase creation, and overlay techniques were applied using ArcGIS 10 software (ESRI) to facilitate shoreline extraction analysis.

3.1.1. Image treatment / Obrada slika

The technique for processing aerial photographs involves three main steps: digitizing, rectifying, and mosaicing the images. The aerial photos were digitized and scanned using

an A3 scanner with a resolution of 1000 dpi. However, these images can exhibit various distortions that may introduce errors of several meters.

Geometric corrections were applied to the aerial photographs using ERDAS Imagine 9.2 software [29] to reduce distortions caused by tilt, scale, and orientation. These operations were conducted by the National Institute of Cartography and Remote Sensing (INRS) and relied on the use of Ground Control Points (GCPs). A total of 35 GCPs were selected to georeference the aerial photographs. The images were georeferenced using the projection system UTM, WGS 1984, Zone 31 [21]. The resulting images were then combined into a single image and stored in TIFF format.

Our study area is located in a micro-tidal zone, where the tidal variation between low and high tide generally ranges from 60 to 70 cm. To minimize errors associated with tidal variations, multi-date images were collected during periods of high tide [30-31].

3.1.2. Shoreline Extraction and error estimation / Ekstrakcija obalne linije i procjena pogreške

The annual rates of shoreline change in our study area over the past twenty years were assessed using the Digital Shoreline Analysis System (DSAS), developed by the United States Geological Survey (USGS), and incorporated into ArcGIS 10. This approach allowed us to evaluate both short-and long-term variations in the shoreline [32].

The Digital Shoreline Analysis System (DSAS) estimates the shoreline position for each transect by generating 720 cross-shore transects, each 250 m long, spaced every 20 m along the baseline. (Figure 3).

For our analysis, we utilize two statistical outcomes generated by the DSAS model [33]: (1) the Endpoint Rate (EPR) and (2) the Net Shoreline Movement (NSM).

Table 1 Data used to measure shoreline evolution between Sidi Madjedoub and Oureah
Tablica 1. Podaci korišteni za mjerenje evolucije obale između Sidi Madjedouba i Oureaha

Date	Data source	Scale	File type
2003	Aerial photos	1/10000	Geo-Tiff
2014	Satellite image (QuickBird)	0.5 m resolution	Raster (Geo-Tiff)
2023	Satellite image (QuickBird)	0,5 m resolution	Raster (Geo-Tiff)

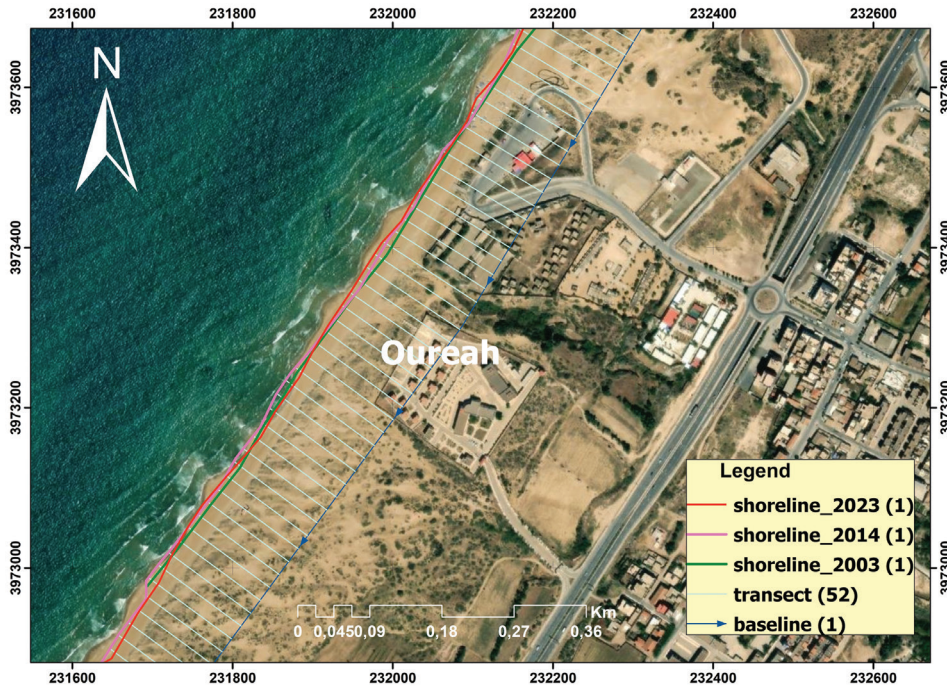


Figure 3 Transect mapping
Slika 3. Mapiranje transekata

The End Point Rate (EPR) is determined by dividing the distance between the old and recent shorelines by the time interval between them (Eq. 1). The EPR is expressed in meters per year (m/year) and is a technique commonly employed by researchers [34].

$$EPR \text{ (m/year)} = \frac{D_1 - D_2}{t_1 - t_0} \quad (1)$$

- D_1 and D_2 : distance between the old and recent shoreline.
- t_0 and t_1 : the dates associated with the two shoreline positions.

The second technique, the Net Shoreline Movement (NSM) method, measures the distance between the most recent and oldest shorelines for each transect [35]. After calculating the accretion and erosion rates for our study area, we created seven classes [35] (Table 2).

Table 2 Classification of shorelines change according to EPR [36]
Tablica 2. Klasifikacija promjene obalnih linija prema EPR-u (stopi krajnje točke)

Rate of shoreline change (m/year)	Shoreline classification	
1	>2	Very high erosion
2	>-1 and <-2	High erosion
3	-1> and < 0	Moderate erosion
4	0	Stable
5	> 0 and < +1	Moderate accretion
6	> +1 and < +2	High accretion
7	> +2	Very high accretion

Table 3 Evaluation of measurement errors for each source of coastal data
Tablica 3. Procjena pogrešaka mjerenja za svaki izvor obalnih podataka

Estimated uncertainty	2003	2014	2023
uncertainty of digitization (U_d)	±3 m	±3 m	±3 m
Uncertainty of pixel (U_p)	±1 m	±1 m	±1 m
Uncertainty of georeferencing (U_g) RMSE of ortho-rectification	±4,9 m	±2,5 m	±2,5 m
the uncertainty of tide level positioning at the time of aerial photography (U_{pd})	±0,5 m	±0,5 m	±0,5 m
The total uncertainty (U_t) (m)	5,85	4,06	4,06
The weights (w_i)	0.55	0.45	0.45
total weighted uncertainty U_{total}		5.8 m	
Annualized Uncertainty for 20 years (U_a)		0,29 m/year	

According to [37], the results of shoreline changes are not reliable without assessing and measuring error margins (uncertainties). These uncertainties include the geo-referencing error (U_g), pixel error (U_p) [38], digitization error (U_d), and the error related to the tide level at the time the aerial photograph was taken (U_{pd}). The total uncertainty (U_t) is calculated as the square root of the sum of the squares of these variables (Eq. 2) [39-40].

$$U_t \text{ (m)} = \sqrt{U_g^2 + U_p^2 + U_d^2 + U_{pd}^2} \quad (2)$$

The total weighted uncertainty U_a (m/year) is computed by weighting the uncertainties U_{t1} , U_{t2} and U_{t3} ... according to the length of the periods L_1 , L_2 and L_3 . The weights (w_i) are defined as (Eq. 3):

$$w_i = \frac{L_i}{\sum_1^3 L_j} \quad (3)$$

where:

L_1 is the length of the period ($L_1 = 2014 - 2003$, $L_2 = 2023 - 2014$ and $L_3 = 2023 - 2003$).

$\sum_1^3 L_j$ is the total length of all periods (20 years).

The total weighted uncertainty U_{total} is then calculated as: (Eq. 4):

$$U_{total} = \sqrt{w_1 * U_{t1} + w_2 * U_{t2} + w_3 * U_{t3}} \quad (4)$$

In this study, the annualized degree of uncertainty (U_a) over a period of twenty years is equal to 0.29 m/year (Table 3).

3.2. Waves Modeling / Modeliranje valova

In this study, we analyze the effects of wave climate on shoreline stability. Wave propagation modeling is used to examine wave dynamics in shallow water [41]. The spectral wave model MIKE 21-SW was employed to simulate wave propagation and evaluate the pattern of wave energy distribution along the coast. This model includes one land boundary and three open boundaries [42].

The data input for the MIKE 21 spectral wave model (SW) includes significant wave height (Hs), tide, peak wave period (T_p) (Table 4), directional standard deviation, bathymetry data, wind direction [42]. Two parameters were considered to configure the SW module: bottom friction and breaking wave. The bottom friction was set to a value of 0.04, while the breaking wave parameter was set to 0.8.

MIKE21 SW uses a cell-centered finite-volume method to solve the differential equations that govern wave dynamics. The governing equations in MIKE21 SW are presented in both polar and Cartesian coordinates [43-44], as detailed below: Eq. (5).

$$\frac{S}{\sigma} = \frac{\partial N}{\partial t} + \nabla(\vec{v}N) \quad (5)$$

Where *N* represents the action density over time *t*, expressed as $N = \frac{E}{\sigma}$, where *E* represents the wave energy density and σ is the wave frequency. $\frac{S}{\sigma}$ is the source term accounting for energy changes due to wind input, non-linear interactions and dissipation. The expression $\nabla(\vec{v}N)$ represents the divergence of wave action flux.

Bathymetric variation is a crucial factor in the propagation of swell and the dissipation of wave energy. The bathymetric data used for MIKE 21-2D was obtained from GEBCO and a digital bathymetric map from Navionics for the year 2020, using the WGS84 coordinate system with UTM projection in Zone 31. This data was processed in Mike Zero under the "Mesh Generator" module from the Danish Hydraulics Institute (DHI);

it was interpolated onto unstructured triangular meshes. A fine mesh was employed near the coastline, while a larger mesh was used for the offshore zone (Figure 4).

By analyzing the annual wave rose (Figure 2) and the orientation of Sidi Madjedoub coast's, extending from the east to Oureah in the west, the studied coastline is principally exposed to waves from the north-northeast (22.5°), northwest (315°), and west (270°) (Table 4).

Table 4 Forcing conditions and Boundary input
Tablica 4. Prisilni uvjeti i granični parametri

Parameters	waves directions		
	north-northeast 22.5°	northwest 315°	west 270°
Hs (m)	5.44	5.16	4.72
Peak period (s)	8.10	8.00	8.25

4. RESULTS / Rezultati

4.1. DSAS Results / DSAS rezultati

This study analyzes the evolution of the shoreline along the coast from Sidi Majdoub to Oureah Beach using automated calculation methods. The results obtained are presented in Figures 5, 6, and 7 for the following periods: 2003-2014, 2014-2023, and 2003-2023, additionally, the shoreline evolution rates along the coast are listed in Table 5.

DSAS generated 720 transects perpendicular to the baseline, spaced at 20-meter intervals along a 15-kilometer stretch of coastline. For a comprehensive diachronic analysis, the study area is subdivided into three segments: (east, center, and west).

The first sector, located between Sidi Madjedoub Beach and Metarba Beach, includes 181 transects. The second sector, situated between Corniche Cliffs and Crique Beach, comprises 165 transects. Finally, the last sector, extending from Sablette Cliffs to Oureah Beach, comprises 304 transects.

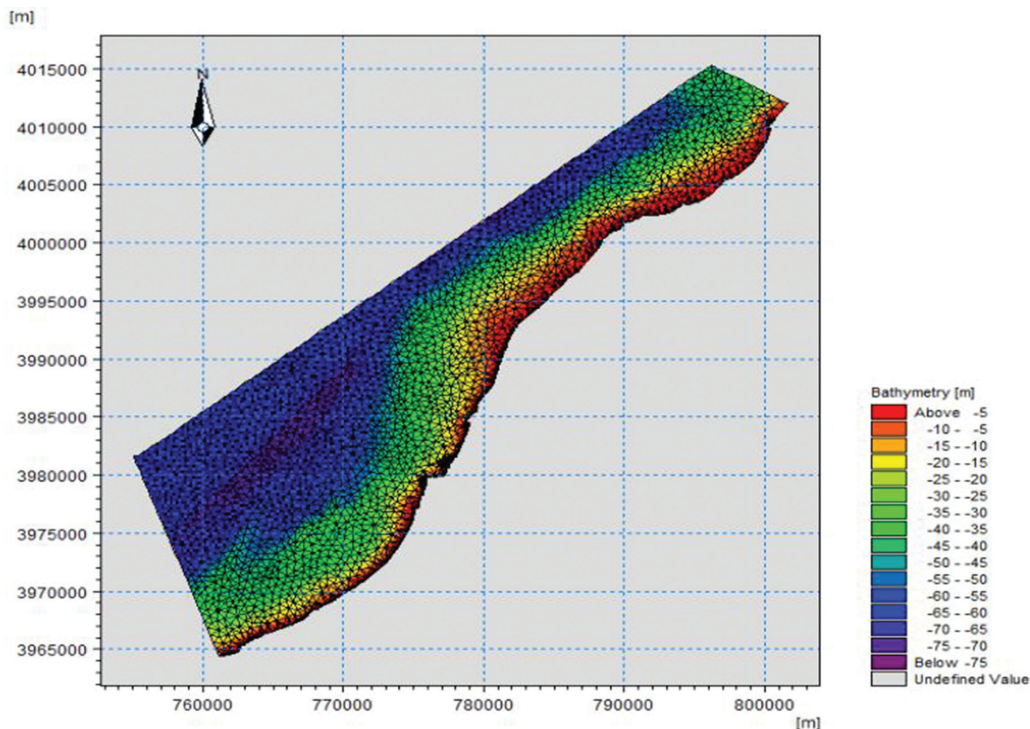


Figure 4 Triangular mesh of the study area
Slika 4. Trokutasta mreža područja istraživanja

Period 2003-2014 / Razdoblje 2003. – 2014.:

During the period between 2003 and 2014 (11 years), the coastal zone between Sidi Madjedoub Beach to Oureah Beach experienced important erosion, affecting over 85% of the study area (Figure 5). The global evolution of shoreline indicated that all transects in the studied region (west, centre, and east) were exposed to high erosion, with a mean rate of -0.8 m/year. During this period, the most important regression was registered on the sandy beaches of the region (Sidi Madjedoub, Metarba, Salamander, Crique, and Sablette west), reaching rates of up to -20 m/year.

a. Period 2014-2023 / Razdoblje 2014. – 2023.:

During the period between 2014 and 2023 (09 years), the coastal zone between Sidi Madjedoub Beach to Oureah Beach indicated a situation of progression-regression-progression compared to the period from 2003 to 2014 (Figure 6). The progression of the shoreline is more important in the eastern segment of the study area (East Sidi Madjedoub), with a range of variation between -23 and +24 meters and an annual rate ranging from -2.65 to +2.73 m/year. A maximum accretion rate is noted on Metarba East beach. This state of accretion

can be explained by the impact of coastal protection structures (breakwaters and groins) installed in the central part since 2012, which have resulted in the formation of "tombolos"

b. Period 2003-2023 / Razdoblje 2003. – 2023.:

The results obtained from the analysis of the global evolution of shoreline changes over the last 20 years (2003–2023) indicate that almost all the transects in the studied region (west, center, and east) have been exposed to relatively rapid erosion (Figure 7).

In the eastern part, the average rates of erosion calculated using the EPR method vary between -12.01 m/year and +2.8 m/year, with a mean erosion rate of -0.28 m/year. The highest erosion rate is registered at Sidi Madjedoub beach, with an EPR rate of -4 m/year.

In the central part, between the Corniche cliffs and Crique beach, the shoreline fluctuates between accretion and retreat, with a rate of change of -0.29 m/year, along with a maximum erosion rate observed at the Corniche cliffs.

In the western part, between Crique beach and Stidia beach, the shoreline shows a relatively stable situation compared to the eastern and central parts, with an average rate of -0.13 m/year.

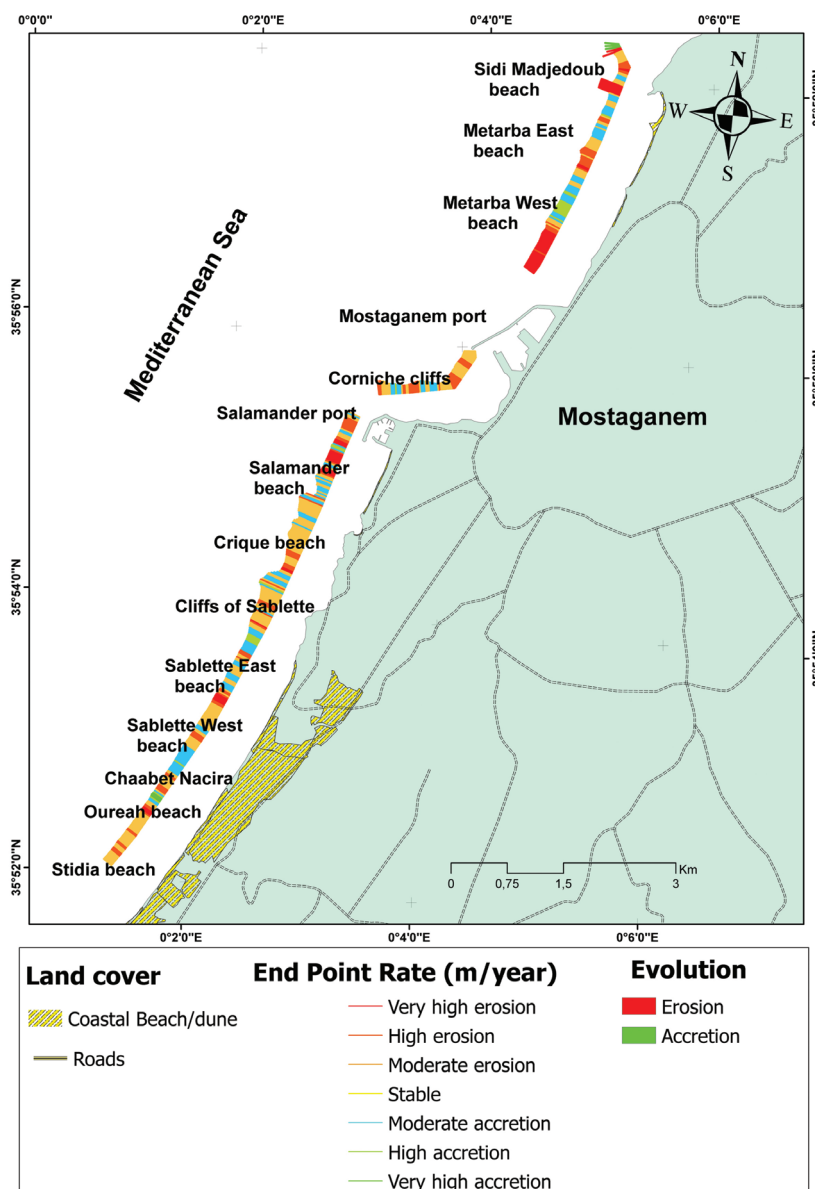


Figure 5 Analysis of the shoreline change between 2003 and 2014 in the study area
Slika 5. Analiza promjene obalne linije između 2003. i 2014. na području istraživanja

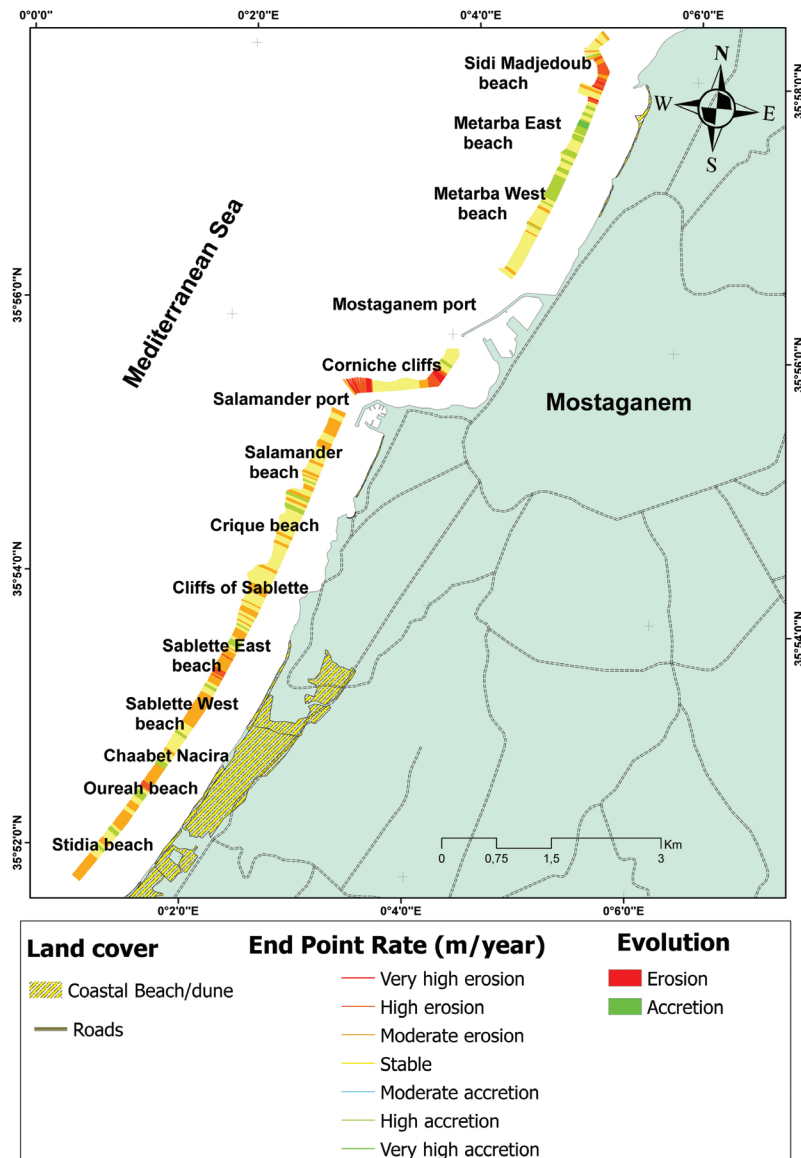


Figure 6 Analysis of the shoreline change between 2014 and 2023 in the study area
Slika 6. Analiza promjene obalne linije između 2014. i 2023. na području istraživanja

Table 5 Long-term shoreline change rates
Tablica 5. Stope dugoročnih promjena obalne linije

Sector ID	Number of transects	coastal zone	Mean shoreline change (m/year)	High Erosion (m/year)	High Accretion (m/year)
Eastern part	1 to 65	Sidi Madjedoub beach	-1.6	-11.98	+0.98
	66 to 94	Metarba East beach	0.59	-0.06	+1.32
	95 to 181	Metarba West beach (Moulin bigour)	-0.07	-2.08	+1.34
Center part		Mostaganem port		Unmeasured Zone	
	248 to 335	Corniche Cliffs	-0.49	-2.68	+0.7
		Salamander port		Unmeasured Zone	
	351 to 405	Salamander beach	-0.39	-1.25	+0.67
Western part	406 to 413	Crique beach	+0.01	-0.52	+0.4
	414 to 503	Cliffs of Sablette	-0.05	-0.73	+0.87
	504 to 531	Sablette East beach	+0.08	-1.12	+0.9
	532 to 603	Sablette West beach	-0.34	-0.99	+0.61
	604 to 653	Chaabet Nacira beach	+0.02	-0.94	+0.78
	654 to 690	Oureah beach	-0.25	-0.81	+0.29
	691 to 717	Stidia beach	-0.25	-0.98	+0.87

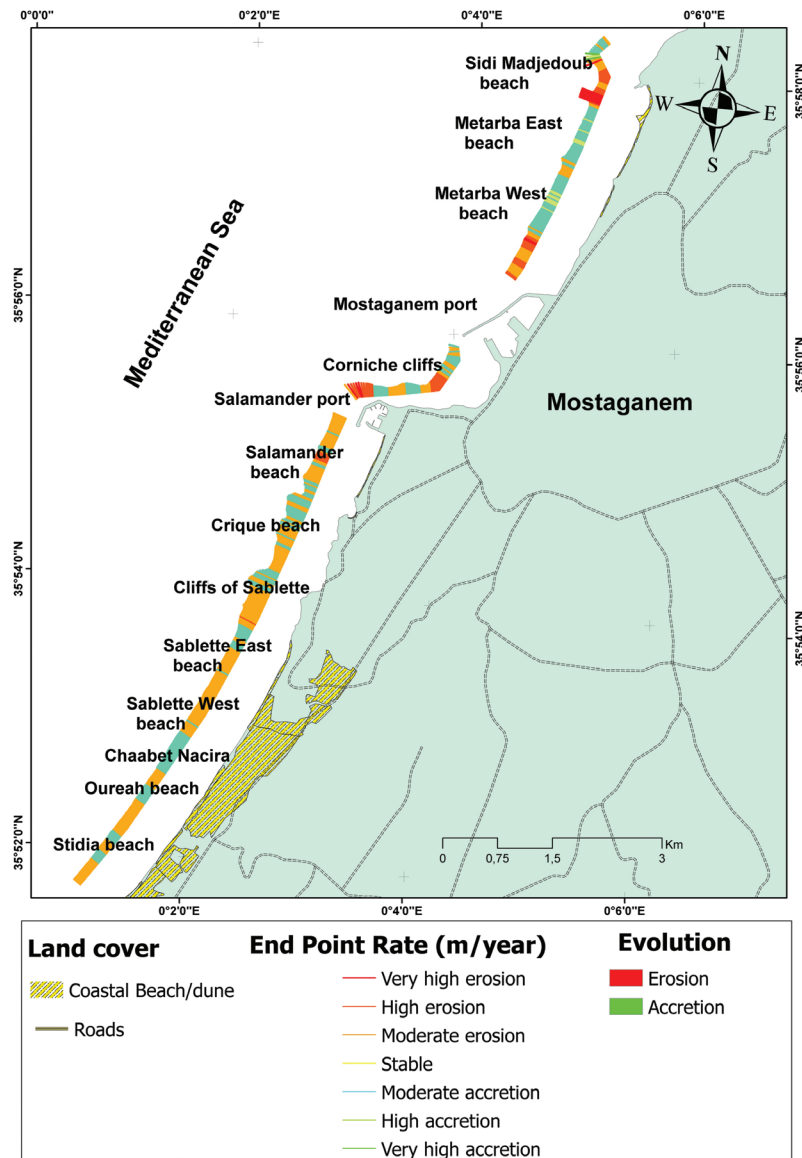


Figure 7 Analysis of the shoreline change between 2003 and 2023 in the study area
 Slika 7. Analiza promjene obalne linije između 2003. i 2023. na području istraživanja

4.2. Numerical modelling of waves / Numeričko modeliranje valova

This part aims to show the wave propagation towards the coast to show their contribution on the shoreline morphology; the three relevant sector discussed before are analysed.

Analysis of the results shows that north-northeast (22.5°) waves (Figure 8) have the highest amplitude, particularly apparent during spring storms in the study area. These waves grow toward the coast at a diagonal angle. These waves do not keep their initial energy due to the addition of refraction and depth-induced breaking phenomena. The wave heights decrease to low values in the shallow water, ranging from 0.42 meters to 1.2 meters on sandy beaches and from 0.1 m to 2.2 meters in front of the harbor's jetty and cliffs area. The refraction coefficients vary between 0.08 and 0.7; these waves generate rip currents.

Figure 9 shows the propagation of waves from the northwest sector, the wave heights values near the coast vary between 0.8 and 1.6 meters, and refraction coefficients vary between 0.11 and 0.37. In front of the studied area, refraction is less important because the crests of the northwesterly waves run parallel to the bathymetric contours. However, in front of the cliffs area and jetties significant wave heights reach 3.2 m; in this case, the energy dissipation is principally caused by diffraction phenomena.

The waves from the western sector (270°) (Figure 10) are generally winter waves. Significant wave heights decrease considerably, with values ranging between 0.2 meters and 1.5 meters and refraction coefficients varying between 0.08 and 0.83 across the study area. The lowest wave heights are observed along sandy coasts such as Sablette and Oureah while the highest values are observed approximately harbor's jetty.

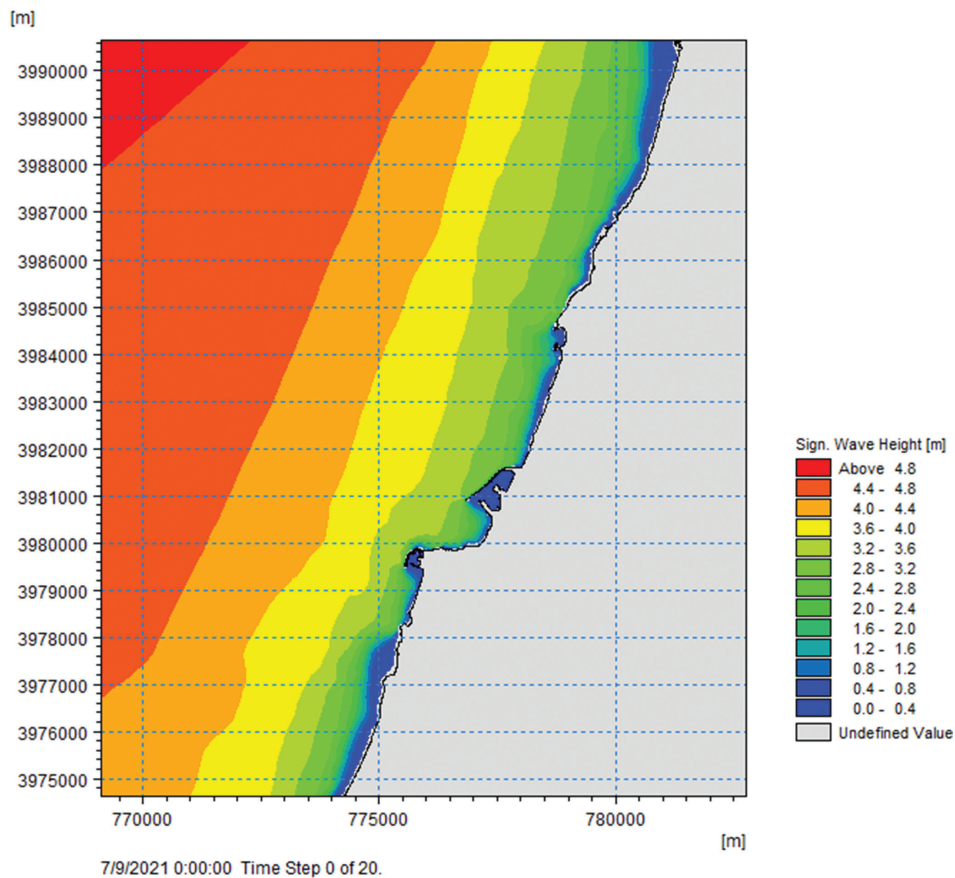


Figure 8 Propagation of north-northeast waves offshore (22.5°) simulated by Mike 21_SW model
 Slika 8. Širenje sjeverno-sjevernoistočnih valova od obale (22,5°) simulirano modelom Mike 21_SW

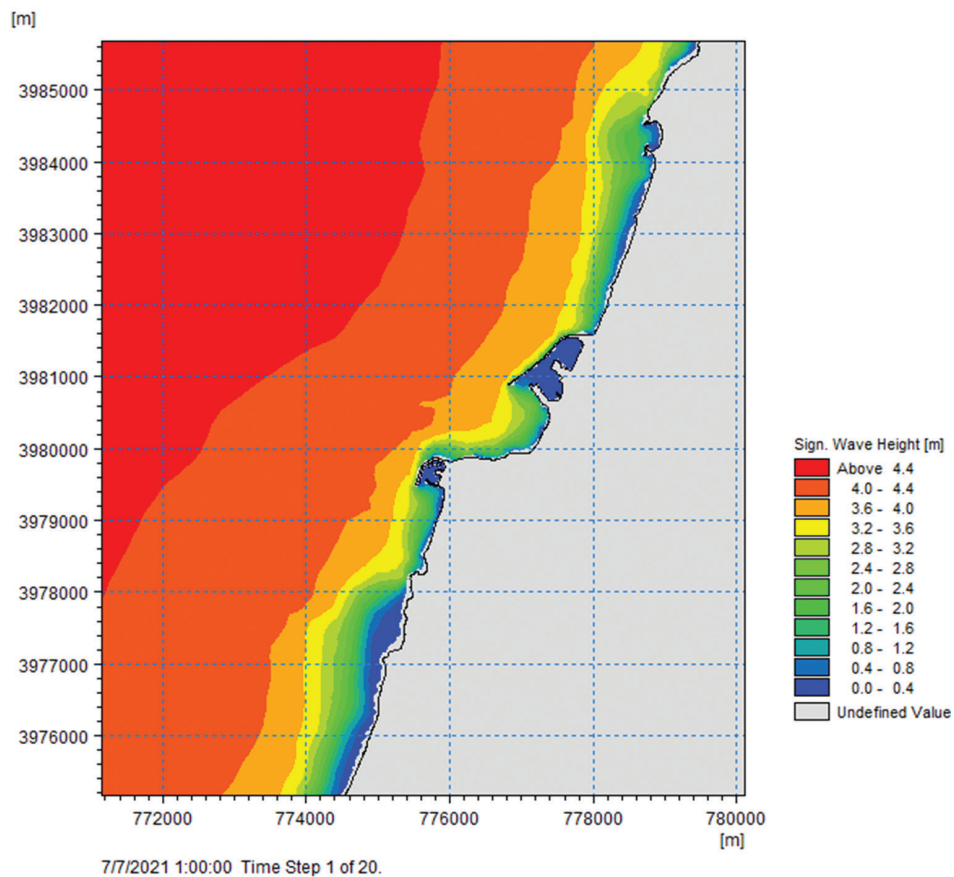


Figure 9 Propagation of northwest waves offshore (315°) simulated by Mike 21_SW model
 Slika 9. Širenje sjeverozapadnih valova od obale (315°) simulirano modelom Mike 21_SW

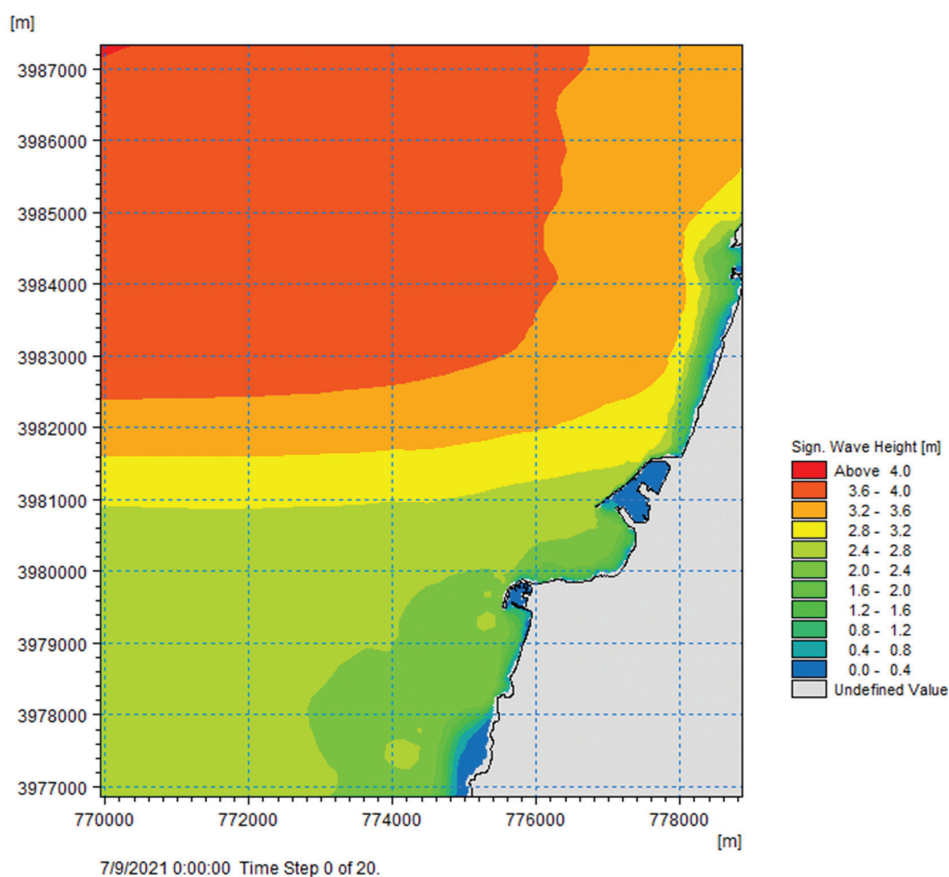


Figure 10 Propagation of west waves offshore (270°) simulated by Mike 21_SW model
 Slika 10. Širenje zapadnih valova od obale (270°) simulirano modelom Mike 21_SW

5. DISCUSSION / Rasprava

According to these results, the analysis of shoreline evolution over the past 20 years (2003–2023) indicates that our study area is exposed to either erosion or accretion, depending on the part. Additionally, the results show that 62% of the coastline has experienced erosion, while 38% has experienced accretion.

The spatio-temporal dynamics of the shoreline, from Sidi Madjedoub Beach in the east to Oureah Beach in the west, can be attributed to natural factors, such as coastal geomorphology, swells, currents, and storms, as well as human activities, including urbanization, the Mostaganem and Salamander ports, tourism infrastructure, coastal economic activities, illegal sand mining, and coastal engineering.

The coastal sector from Sidi Madjedoub to Oureah, with its orientation, morphology, and the width of the continental shelf open to the northwest, indicates that the study area is more affected by waves from the north-northeast than by those from the northwest.

The relationship between coastline formation and wave action has been illustrated in numerous studies [45]. Results from wave simulations show that waves arriving from the north-northeast direction approach the shore at an oblique angle, generating alongshore drift in the south-southwest direction. This drift may contribute to sediment movement in the eastern part of the study area (e.g., Metarba, Sidi Madjedoub, and the Corniche cliffs), where shoreline retreat has been observed, with average rates of -21.56 m, -42.47 m, and -11.51 m, respectively.

This situation changed slightly during the period from 2018 to 2021 in the Corniche cliffs area, where the Ministry of Public Works and Basic Infrastructure built a retaining wall during this period with a length of 400 metres [46].

The results of the Mike 21 model were compared to the results edited by the model calibrated by Amarouche and al [47–48]. This study showed a coherent distribution between the referenced data [47–48] and simulation results for significant wave height. The calibrated data show that significant wave heights vary between 0.21 and 0.4 metres in the very shallow water in the study area.

One of the elements controlling sediment dynamics in this region is the construction of the Mostagnem port (Figure 11.a) and Salamander port, which may have modified local sediment dynamics. This structure can modify wave's conditions on the beaches of Sidi Madjedoub and Metarba. The rotation of waves around the breakwater of the main jetty at the port results in the formation of a return current that transported sediment from these beaches to offshore areas. To solve this problem, a groyne and a breakwater were installed at Sidi Madjedoub Beach in 2012 to prevent the dispersion of sediment offshore (Fig. 11.b). However, the limited efficacy of these new coastal defences had resulted in progressive erosion in the western part of Metarba West beach (Fig. 11.c).

In addition to these factors, human activities in this region, such as sand mining (Fig. 11.d), tourism development (Fig. 11.e), industrial activities, and finally the phenomenon of expansion of urbanisation along the coastal zone (hotels, houses, road) have caused a sediment deficit in this area (Fig. 11.f) [25].



Figure 11 a) Mostaganem port; b) protection structures (01 breakwater); c) coastal erosion and landslide; d) illegal sand mining; e) tourism development; f) Urbanization along the coastal area

Slika 11. a) luka Mostaganem; b) zaštitne strukture (01 lukobran); c) obalna erozija i odroni; d) ilegalno iskopavanje pijeska; e) razvoj turizma; f) urbanizacija duž obalnog područja

6. CONCLUSION / Zaključak

The shoreline evolution along the coastal of Mostaganem Bay over the entire period (2003–2023) was studied by geospatial techniques (DSAS and GIS), additionally, numerical modelling of wave propagation was applied using the Mike 21 model.

The analysis of the spatial-temporal evolutions of the shoreline along the coast from Sidi Madjedoub to Oureah between 2003 and 2023 showed an erosion situation, particularly in the eastern part with a mean rate of retreat of -0.28 m/year. This change is principally due to human intervention by illegal sand mining at the different beaches of the study area (Sidi Madjedoub beach, Sablette beach, and Oureah beach).

The results obtained from the Mike 21 model clearly show waves directed from the north-northeast have the highest amplitude in the study region, with a mean height ranging from 0.1 to 2 meters.

In addition, coastal protection structures (such as groynes, breakwaters) can create local sediment accumulation in the form of tombolos, but also cause erosion in areas adjacent to these constructions.

Indeed, in the study area, several large-scale construction projects were built in coastal zones without taking into account coastal law 02-02, which prohibits this type of structure.

The results obtained would be useful and applicable for the implementation of coastal management plans.

Author Contribution: M. S.: Software, Conceptualization, Investigation, Writing – review and editing; A. E. A. D.: Validation, editing and Resources; K. M.: Methodology, Supervision; Y. S. C.: review and Resources

Funding: Not applicable.

Conflict of interest: We have no conflict of interest

Acknowledgements: We would like to thank especially INCT providing additional data for this study.

REFERENCES / Literatura

- Ennouali, Z., Fannassi, Y., Lahssini, G., Benmohammadi, A., & Masria, A. (2023). Mapping Coastal vulnerability using machine learning algorithms: A case study at North coastline of Sebou estuary, Morocco. *Regional Studies in Marine Science*, 60, 102829. <https://doi.org/10.1016/j.rsma.2023.102829>
- Surić, M. (2009). Rekonstruiranje promjena morske razine na istočnoj obali Jadrana (Hrvatska) – pregled. *Geoadria*, 14 (2), 181-199. <https://doi.org/10.15291/geoadria.550>
- Tahri, M., Maanan, M., Maanan, M., Bouksim, H., & Hakdaoui, M. (2017). Using Fuzzy Analytic Hierarchy Process multi-criteria and automatic computation to analyse coastal vulnerability. *Progress in Physical Geography*, 41 (3), 268-285. <https://doi.org/10.1177/0309133317695158>
- Boukhennaf, A., & Mezouar, K. (2023a). Long and short-term evolution of the Algerian coastline using remote sensing and GIS technology. *Regional Studies in Marine Science*, 61, 102893. <https://doi.org/10.1016/j.rsma.2023.102893>
- Otmani, H., Belkessa, R., Bengoufa, S., Boukhediche, W., Djerrai, N., & Abbad, K. (2020). Assessment of shoreline dynamics on the Eastern Coast of Algiers (Algeria): A spatiotemporal analysis using in situ measurements and geospatial tools. *Arabian Journal of Geosciences*, 13, 1-15. <https://doi.org/10.1007/s12517-020-05961-5>; <https://doi.org/10.1007/s12517-020-5069-6>
- Fagherazzi, S., Mariotti, G., Wiberg, P. L., & McGlathery, K. J. (2013). Marsh collapse does not require sea level rise. *Oceanography*, 26 (3), 70-77. <https://doi.org/10.5670/oceanog.2013.45>
- Fletcher, C., Rooney, J., Barbee, M., Lim, S.-C., & Richmond, B. (2003). Mapping shoreline change using digital orthophotogrammetry on Maui, Hawaii. *Journal of coastal research*, 38 (38), 106-124. <https://www.jstor.org/stable/i25736593>
- Hereher, M. E. (2015). Coastal vulnerability assessment for Egypt's Mediterranean coast. *Geomatics Natural Hazards and Risk*, 6 (4), 342-355. <https://doi.org/10.1080/19475705.2013.845115>
- Mahapatra, M., Ratheesh, R., & Rajawat, A. (2014). Shoreline change analysis along the coast of South Gujarat, India, using digital shoreline analysis system. *Journal of the Indian Society of Remote Sensing*, 42, 869-876. <https://doi.org/10.1007/s12524-013-0334-8>
- Mbezi, J., Mango, J., Lubida, A., Valerian, R., & Kato, L. (2024). Exploring shoreline changes and their implications in coastal communities using GIS and remote sensing techniques: The case of eastern beaches of Unguja island, Tanzania. *Regional Studies in Marine Science*, 75, 103566. <https://doi.org/10.1016/j.rsma.2024.103566>
- Zaghden, H., Serbaji, M. M., Saliot, A., & Sayadi, S. (2016). The Tunisian Mediterranean coastline: potential threats from urban discharges Sfax-Tunisian Mediterranean coasts. *Desalination and Water Treatment*, 57 (52), 24765-24777. <https://doi.org/10.1080/19443994.2016.1149107>
- Mociu, N. C. (2021). A Study on the Urban Redevelopment of Ovidius's Shoreline. *Ovidius University Annals of Constanta-Series Civil Engineering*, 23 (1), 133-138. <https://doi.org/10.2478/ouacscce-2021-0017>

- [13] Szymczak, E., & Rucińska, M. (2021). Characteristics of morphodynamic conditions in the shallows of Puck Bay (southern Baltic Sea). *Oceanological and Hydrobiological Studies*, 50 (2), 220-231. <https://doi.org/10.2478/oandhs-2021-0019>
- [14] Baral, R., Pradhan, S., Samal, R. N., & Mishra, S. K. (2018). Shoreline change analysis at Chilika Lagoon Coast, India using digital shoreline analysis system. *Journal of the Indian Society of Remote Sensing*, 46 (10), 1637-1644. <https://doi.org/10.1007/s12524-018-0818-7>
- [15] Dobrică, G., Cerneagă, C., & Maftai, C. (2022). Shoreline Change Analysis Using Digital Shoreline Analysis System along Southeast Romanian Coast. In *Recent Research on Geomorphology, Sedimentology, Marine Geosciences and Geochemistry: Proceedings of the 2nd Springer Conference of the Arabian Journal of Geosciences (CAJG-2)*, Tunisia 2019, pp. 81-83. Springer International Publishing. https://doi.org/10.1007/978-3-030-72547-1_18
- [16] Ramnalis, P., Batzakis, D.-V., & Karymbalis, E. (2023). Applying two methodologies of an integrated coastal vulnerability index (ICVI) to future sea-level rise. Case study: southern coast of the Gulf of Corinth, Greece. *Geoadria*, 28 (1), 1-24. <https://doi.org/10.15291/geoadria.4046>; <https://doi.org/10.15291/geoadria.4234>
- [17] Belibassakis, K. A., & Karathanasi, F. E. (2017). Modelling nearshore hydrodynamics and circulation under the impact of high waves at the coast of Varkiza in Saronic-Athens Gulf. *Oceanologia*, 59 (3), 350-364. <https://doi.org/10.1016/j.oceano.2017.04.001>
- [18] Esmail, M., Mahmood, W. E., & Fath, H. (2019). Assessment and prediction of shoreline change using multi-temporal satellite images and statistics: Case study of Damietta coast, Egypt. *Applied Ocean Research*, 82, 274-282. <https://doi.org/10.1016/j.apor.2018.11.009>
- [19] Gireesh, B., Acharyulu, P. S. N., CH, V., Sivaiah, B., Venkateswararao, K., Prasad, K. V. S. R., & Naidu, C. V. (2023). Extraction and mapping of shoreline changes along the Visakhapatnam-Kakinada coast using satellite imageries. *Journal of Earth System Science*, 132 (2), 52. <https://doi.org/10.1007/s12040-023-02052-x>
- [20] Görmüş, T., Ayat, B., Aydoğan, B., & Tütü, F. (2021). Basin scale spatiotemporal analysis of shoreline change in the Black Sea. *Estuarine, Coastal and Shelf Science*, 252, 107247. <https://doi.org/10.1016/j.ecss.2021.107247>
- [21] Ayadi, K., Boutiba, M., Sabatier, F., & Guettouche, M. S. (2016). Detection and analysis of historical variations in the shoreline, using digital aerial photos, satellite images, and topographic surveys DGPS: case of the Bejaia bay (East Algeria). *Arabian Journal of Geosciences*, 9, 1-12. <https://doi.org/10.1007/s12040-023-02052-x>
- [22] Bengoufa, S., Niculescu, S., Mihoubi, M. K., Belkessa, R., Rami, A., Rabehi, W., & Abbad, K. (2021). Machine learning and shoreline monitoring using optical satellite images: case study of the Mostaganem shoreline, Algeria. *Journal of applied remote sensing*, 15 (2), 026509-026509. <https://doi.org/10.1117/1.JRS.15.026509>
- [23] Boukhennaf, A., & Mezouar, K. (2023b). Long and short-term evolution of the Algerian coastline using remote sensing and GIS technology. *Regional Studies in Marine Science*, 102893. <https://doi.org/10.1016/j.rsma.2023.102893>
- [24] Kermani, S., Boutiba, M., Guendouz, M., Guettouche, M. S., & Khelfani, D. (2016). Detection and analysis of shoreline changes using geospatial tools and automatic computation: Case of jijelian sandy coast (East Algeria). *Ocean & coastal management*, 132, 46-58. <https://doi.org/10.1016/j.ocecoaman.2016.08.010>
- [25] Senouci, R., & Taïbi, N.-E. (2019b). Impact of the Urbanization on Coastal Dune: Case of Kharrouba, West of Algeria. *Environnements*, 4 (1), 90-98. DOI: 10.12957/jse.2019.39951
- [26] Senouci, R., Taïbi, N.-E., Teodoro, A. C., Duarte, L., Mansour, H., & Yahia Meddah, R. (2021). GIS-based expert knowledge for landslide susceptibility mapping (LSM): case of mostaganem coast district, west of Algeria. *Sustainability*, 13 (2), 630. <https://doi.org/10.3390/su13020630>
- [27] Infoplaza Marin database (1992-2021). www.waveclimate.com
- [28] Kaddour, S., Hemdane, Y., Kessali, N., Belabdi, K., & Sallaye, M. (2022). Study of Shoreline Changes Through Digital Shoreline Analysis System and Wave Modeling: Case of the Sandy Coast of Bou-Ismaïl Bay, Algeria. *Ocean Science Journal*, 57 (3), 493-527. <https://doi.org/10.1007/s12601-022-00083-x>
- [29] Farah, T., Taïbi, N.-E., & Chouieb, M. (2022). Evolution of Land Cover in the Traras MTS. Region Between 1984 and 2020 by Remote Sensing and Gis (Northwest Algeria). *Ekológia (Bratislava)*, 41 (4), 375-385. <https://doi.org/10.2478/eko-2022-0038>
- [30] Ngowo, R. G., Ribeiro, M. C., & Pereira, M. J. (2021). Quantifying 28-year (1991–2019) shoreline change trends along the Mnazi Bay–Ruvuma Estuary Marine Park, Tanzania. *Remote Sensing Applications: Society and Environment*, 23, 100607. <https://doi.org/10.1016/j.rsase.2021.100607>
- [31] Martinez del Pozo, J., & Anfuso, G. (2008). Spatial Approach to Medium-term Coastal Evolution in South Sicily (Italy): Implications for Coastal Erosion Management. *Journal of Coastal Research*, 24(1), 33-42. <https://doi.org/10.2112/05-0598.1>
- [32] Islam, M. S. (2020). Assessing the dynamics of land cover and shoreline changes of Nijhum Dwip (Island) of Bangladesh using remote sensing and GIS techniques. *Regional Studies in Marine Science*, 41, 101578. <https://doi.org/10.1016/j.rsma.2020.101578>
- [33] Sarwar, M. G. M., & Woodroffe, C. D. (2013). Rates of shoreline change along the coast of Bangladesh. *Journal of Coastal Conservation*, 17 (3), 515-526. <https://doi.org/10.1007/s11852-013-0251-6>
- [34] Natesan, U., Parthasarathy, A., Vishnunath, R., Kumar, G. E. J., & Ferrer, V. A. (2015). Monitoring longterm shoreline changes along Tamil Nadu, India using geospatial techniques. *Aquatic Procedia*, 4, 325-332. <https://doi.org/10.1016/j.aqpro.2015.02.044>
- [35] Kumar, L., Afzal, M. S., & Afzal, M. M. (2020). Mapping shoreline change using machine learning: a case study from the eastern Indian coast. *Acta Geophysica*, 68 (4), 1127-1143. <https://doi.org/10.1007/s11600-020-00454-9>
- [36] Morton, R. A., Miller, T. L., & Moore, L. J. (2004). *National assessment of shoreline change: Part 1 Historical shoreline changes and associated coastal land loss along the US Gulf of Mexico*. US Geological Survey. <https://doi.org/10.3133/ofr20041043>
- [37] Millot, C., & Taupier-Letage, I. (2005). Circulation in the Mediterranean sea. *The Mediterranean Sea*, 29-66. <https://doi.org/10.1007/b107143>
- [38] Jonah, F. E., Boateng, I., Osman, A., Shamba, M. J., Mensah, E. A., Adu-Boahen, K., Effah, E. (2016). Shoreline change analysis using end point rate and net shoreline movement statistics: An application to Elmina, Cape Coast and Moree section of Ghana's coast. *Regional Studies in Marine Science*, 7, 19-31. <https://doi.org/10.1016/j.rsma.2016.05.003>
- [39] Mezouar, K., Cherif, Y. S., & Sallaye, M. (2021). Coastal processes and nearshore hydrodynamics under high contrast wave exposure, Bateau-cassé and Stamboul coasts, Algiers Bay. *Estuarine, Coastal and Shelf Science*, 250, 107169. <https://doi.org/10.1016/j.ecss.2021.107169>
- [40] Thieler, E. R., & Danforth, W. W. (1994). Historical shoreline mapping (I): improving techniques and reducing positioning errors. *Journal of Coastal Research*, 549-563. <https://www.jstor.org/stable/4298252>
- [41] Salem Cherif, Y., Mezouar, K., Guerfi, M., Sallaye, M., & Dahmani, A. E. A. (2019). Nearshore hydrodynamics and sediment transport processes along the sandy coast of Boumerdes, Algeria. *Arabian Journal of Geosciences*, 12, 1-17. <https://doi.org/10.1007/s12517-019-4981-0>
- [42] Kaiser, M. F., Ali, W. A., & Tahan, E. (2019). Modeling of Coastal Processes in the Mediterranean Sea: A Pilot Study on the Entrance of Suez Canal in Egypt. In *Coastal and Marine Environments – Physical Processes and Numerical Modelling*. IntechOpen.
- [43] Young, I. R. (1999). *Wind generated ocean waves*. Elsevier. <http://site.ebrary.com/id/10041464>
- [44] Ibrahim, A. S., El-Molla, A. M. & Hany G. I. A. (2024). Impacts of Coastal Structures on Sediment Transport: A Case Study of Damietta, Egypt. *Nashe more*, 71 (2), 45-53. <https://doi.org/10.17818/NM/2024/2.1>
- [45] Siegle, E., & Asp, N. E. (2007). Wave refraction and longshore transport patterns along the southern Santa Catarina coast. *Brazilian Journal of Oceanography*, 55, 109-120. <https://doi.org/10.1590/S1679-87592007000200004>
- [46] Mezouar, K. (2022). *Rapport sur l'évaluation de la situation initiale de l'indicateur commun 15 d'IMAP "Localisation et étendue des habitats potentiellement affectés par les altérations hydrographiques" pour les zones côtières et marines méditerranéennes de l'Algérie*. Retrieved from: <https://iczmplatform.org/>
- [47] Amarouche, K., Akpınar, A., Bachari, N. E. I., Çakmak, R. E., & Houma, F. (2019). Evaluation of a high-resolution wave hindcast model SWAN for the West Mediterranean basin. *Applied Ocean Research*, 84, 225-241. <https://doi.org/10.1016/j.apor.2019.01.014>
- [48] Amarouche, K., Akpınar, A., Bachari, N. E. I., & Houma, F. (2020). Wave energy resource assessment along the Algerian coast based on 39-year wave hindcast. *Renewable Energy*, 153, 840-860. <https://doi.org/10.1016/j.renene.2020.02.040>